Available online at www.sciencedirect.com

SCIENCE DIRECT®

Earth and Planetary Science Letters 235 (2005) 123–140

EPSL

www.elsevier.com/locate/epsl

The pace of rhyolite differentiation and storage in an 'archetypical' silicic magma system, Long Valley, California

Justin I. Simon[a,*], Mary R. Reid[a,b]

[a]Department of Earth and Space Sciences, UCLA, Los Angeles CA 90095-1567, USA
[b]Department of Geology, Northern Arizona University, Flagstaff, AZ, USA

Received 25 June 2004; received in revised form 28 February 2005; accepted 8 March 2005
Available online 23 May 2005
Editor: K. Farley

Abstract

Time scales of silicic magma processes are an important source of information pertaining to the thermal and mass fluxes through the crust but are difficult to quantify. Here we report ion microprobe ^{238}U–^{206}Pb ages for individual zircons from rhyolites from Long Valley caldera, California, and use these data to refine the relationship of production and storage of the 0.8–2.1 Ma precaldera Glass Mountain (GM) rhyolites to that of the caldera-related Bishop Tuff (BT) rhyolite. We also examine the timing of differentiation in the compositionally zoned BT.

Most zircon crystallization in the 3 studied GM rhyolites occurred in two intervals between 2.0 and 1.7 Ma and between 1.1 and 0.85 Ma. Collectively, they support previous inferences based on Sr isotope considerations that differentiation and crystallization in silicic magmas can precede eruption by hundreds of ky. For the BT, zircons contained in the earlier, more evolved part of the eruption have U contents (mostly >1800–4500 ppm) that are higher than those contained in the later, less evolved part of the eruption (mostly 100's to 2000 ppm). When scarce Mesozoic-aged zircons are excluded, the mean pre-eruption crystallization age for the late BT zircons studied here is about 90 ky older than a 760 ± 2 ka Ar/Ar sanidine eruption age. An identical mean pre-eruption zircon age is obtained for the early part of the BT eruption as well as in an earlier study and implies virtually simultaneous crystallization of compositionally distinct melts.

Based on the largely distinct chemical and age characteristics of the zircon age populations, we conclude that the GM and BT rhyolites record episodes of punctuated and independent evolution rather than the periodic tapping of a long-lived magma chamber. Sr isotope characteristics of BT minerals previously used to support inheritance of those minerals from GM magmas can be explained by radiogenic ingrowth and by crystal growth from isotopically heterogeneous domains in the nascent BT magma chamber; evidence for the latter is provided by anomalously radiogenic feldspars.
© 2005 Elsevier B.V. All rights reserved.

Keywords: Long Valley caldera; time scales; rhyolite magmagenesis; ^{238}U–^{206}Pb zircon ages; ion microprobe

* Corresponding author. Tel.: +1 310 206 2940; fax: +1 310 825 2779.
E-mail addresses: jisimon@ucla.edu (J.I. Simon), Mary.Reid@NAU.edu (M.R. Reid).

0012-821X/$ - see front matter © 2005 Elsevier B.V. All rights reserved.
doi:10.1016/j.epsl.2005.03.013

1. Introduction

The mode and pace of silicic magma production is an important component in understanding the formation and evolution of continental crust (cf. [1]). Even allowing for crustal incorporation, mantle-derived magma is a relatively inefficient progenitor of silicic magma. Accumulation times of hundreds to thousands of ky could be required for the more voluminous silicic magmas (100's to 1000's of km^3) if the apparently regular output of rhyolite at many volcanic centers [2] is indicative of steady-state silicic magma production. Silicic magmas can, however, differentiate relatively quickly—and even catastrophically—by, for example, gas-driven filter pressing, gravitational compaction of crystalline material, and/or anatexis of underplated magmas (e.g., [3–5]). Once differentiated, silicic magmas could persist in crystal-dominated ("mushy") states, to be later remobilized for eruption [6]. Rapid production and/or emplacement of rhyolite and sporadic magma storage are supported by geochronologic studies of plutonic rocks (e.g., [7,8]) and by the general observation that crystal ages do not correlate with eruption size in rhyolites [9]. Even if rapidly differentiated, quasi-regular rhyolite production could still be manifest if rate-limited by processes leading up to actual rhyolite differentiation (e.g., [5,10]) and/or by those that interrupt magma storage (e.g., [11,12]).

A salient feature of the caldera system at Long Valley (LV), California, is that rhyolites erupted intermittently for >1 Myr before the climactic eruption. Most studies have, in fact, inferred that the 0.8–2.1 Ma precaldera Glass Mountain (GM) rhyolites (Fig. 1) tapped the same magma body as that responsible for the 0.76 Ma caldera-related Bishop Tuff (BT) (e.g., [13–17]). Discrete model age populations for GM [18] and BT crystals [19,20] as well as progressive evolution of LV magmas towards less evolved compositions [14] could alternately imply that the BT was only the last in a series of differentiation "events". Zircon ages mostly <1 Ma for at least some parts of the BT suggest, moreover, that the rhyolitic magma responsible for the BT may have overlapped in time only the youngest of the GM rhyolites [21]. The system may have been persistently mushy or even at times largely solidified (cf. [7]). Rather than the maturation of a single long-lived magma chamber,

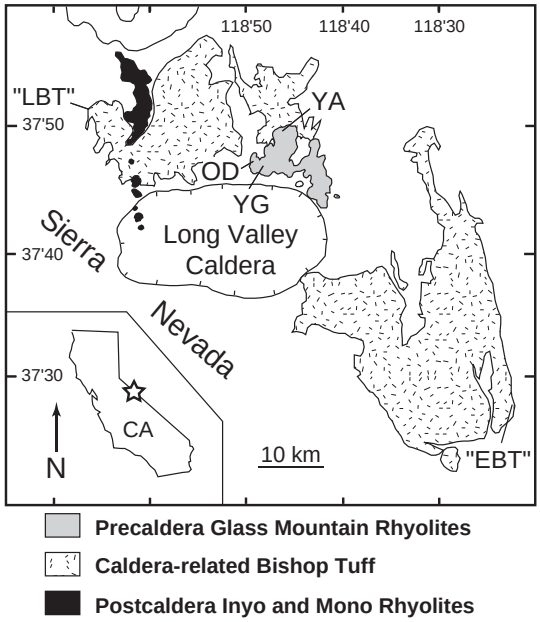

Fig. 1. Map of Long Valley showing sample locations, modified after [31,64]. OD, YG, and YA indicate the location of GM rhyolites within their respective domes. Lines labeled EBT and LBT point to the sampling locations of our early and late Bishop Tuff samples, respectively.

could a protracted silicic volcanic history like that at LV reflect a punctuated history of rhyolite differentiation and, if so, what if any affinity do precaldera rhyolites have to the caldera-forming magma?

The BT and GM suites of rhyolites are compositionally diverse, which could reflect venting of magma systems that underwent internal differentiation [22]. For the BT, compositional zoning has generally been regarded to have developed progressively (e.g., [15,19,23–26]), with more evolved portions stored for hundreds of ky longer than the less evolved portions. If, as suggested above, the BT developed late in the evolutionary history of the GM rhyolites, compositional zonation may have developed in a much shorter time [25]. Existing Sr and Pb model mineral ages for the BT [15,19–21] are permissive of the interpretation that more silicic caps may develop internally in standing magma chambers or even that more and less differentiated portions of silicic magma reservoirs evolve synchronously.

To a large degree, inferences about the relationship of the precaldera GM rhyolites to the caldera-related BT rhyolite and about the timing of differentiation

have relied on model ages and isotopic affinities, the interpretations of which are not unique. Here we present ion microprobe ^{238}U–^{206}Pb ages of ~10^3 μm^3 domains within individual zircons from GM and BT rhyolites. The relatively high liquidus temperature and low settling velocity of zircon in silicic magmas make it an effective tracer of crystallization and crystal carryover from one rhyolite to another [27,28]. The zircon ages enable us to trace the affinities of crystals to different episodes of magmatic activity within the LV system. For the relatively small-volume precaldera rhyolites, we find intervals (~100 to ≥200 ky) of at least intermittent zircon crystallization which confirm and extend results obtained previously for the major mineral phases (e.g., [19]), but which are short with respect to the overall duration of silicic magmatic activity. For more and less evolved portions of the caldera-forming BT, zircons with chemical affinities to their hosts crystallized contemporaneously. This implies simultaneous storage and, in all likelihood, magmatic differentiation of the BT before zircon crystallization. Because the zircon age populations of the rhyolites are largely distinct, we conclude that the precaldera and caldera-forming rhyolites at LV record episodes of punctuated evolution rather than the periodic tapping of a long-lived, silicic magma reservoir.

2. Geologic background and history

Long Valley caldera is located in central California on the eastern flank of the Sierra Nevada at the western boundary of the extensional Basin and Range province (Fig. 1). Jurassic and Cretaceous granitoids of the Sierra Nevada batholith surround the caldera [29]. On the northeast margin of Long Valley caldera reside the precaldera high-silica rhyolites of GM, volcanism that began at ~2.0 Ma and continued episodically until ~0.8 Ma [14,30,31]. Cataclysmic eruption of the caldera-related BT at 0.76 Ma occurred shortly thereafter.

Two GM eruptive episodes have been identified, an older one (~2.0 to ~1.7 Ma) and a younger one (~1.1 to ~0.8 Ma) [30]. Older and younger rhyolites have been further subdivided into inner and outer groups based on their geochemistry and proximity to the Long Valley caldera rim [18,19,24]. The GM effusive lavas are high-silica rhyolites (76.8–77.9 wt.% SiO_2) [30]. Older GM rhyolites contain more crystals (up to 15–20%, typically <10%) than younger rhyolites (up to 6–8%, typically 0–5%) [30]. The caldera-related BT is also a high-silica rhyolite (75–77 wt.% SiO_2) and is zoned in composition and mineralogy, increasing in crystal content from ~5% to ~25% with stratigraphic height [22,23,32].

3. Sample descriptions

Three GM rhyolite samples were chosen that represent the time interval of precaldera magmatism and, for domes YA and YG, that likely have the greatest affinity to the BT magma system. Sample R00LV63 is a crystal-rich perlitic obsidian (15–20% crystals) from the western margin of dome OD. Sample R00LV62 is a dense black crystal-poor vitrophyre (6–7% crystals) from the northwest side of dome YG. Sample JS01LV04 is a dense black crystal-poor vitrophyre (1–2%) from the north central portion of dome YA (Fig. 1).

Two pumice fragments representative of the mineralogical variability in the BT were selected to investigate the generality of results obtained previously for a somewhat limited portion of the BT [21]. The first, R99LV51, is a relatively crystal-rich (~20–25%) pumice fragment (~10 cm in length) from the Mono ignimbrite lobe termed Ig2NW [33] (Fig. 1). Ig2NW yields hotter Fe–Ti temperature estimates and is referred to as "late" BT (LBT) because it is high in the BT stratigraphic sequence. The second, R99LV58, is a crystal-poor (~3–5%) pumice fragment (~15 cm in length) from the distal portion of the Chidago ignimbrite lobe termed Ig1Eb [33] (Fig. 1). Ig1Eb yields cooler Fe–Ti temperature estimates [23] and is referred to as "early" BT (EBT) based on its stratigraphic position. For comparison purposes we reanalyzed the four zircons of EBT plinian fall unit F6 that yielded the greatest age range in an earlier study [21].

4. Analytical methods

The CAMECA ims 1270 ion microprobe at UCLA was used to determine zircon ^{238}U–^{206}Pb crystallization ages, employing established methods (e.g., [34]). Zircons, typically ~100–200 μm in length, were mounted for analyses in two ways. In the first method,

zircons mounted in epoxy were polished to expose their cores. Interior "*core*" and "*near rim*" spot analyses (~25–45 μm in diameter) of the grains were measured. In the second method epoxy-mounted zircon grains were prepared only to expose rim faces. These "*surface*" analyses typically penetrated less than 2 μm.

Individual zircon ages are ^{207}Pb-corrected using a whole rock common ^{207}Pb/^{206}Pb composition of 0.818 [24] (modern surface Pb contamination is minimal). The ^{207}Pb-corrected ages are also adjusted for initial U–Th disequilibrium due to the deficit in radiogenic ^{206}Pb originating from the initial deficit in ^{230}Th relative to ^{238}U [35]. The magnitude of this deficit can be estimated by comparing the Th/U ratios in zircon to those of the host magmas [36] which, in this case, are taken to be those of the Th/U ratios of the whole rocks [14,23]. The absolute effect of this correction (typically +80–90 ky) is accurate to 10 ky, allowing for the range in Th/U ratios observed in Long Valley rhyolites. This correction also assumes in effect that the melts were in secular equilibrium with respect to ^{238}U–^{230}Th when the zircons crystallized, however, the slight ^{230}Th excesses typical of rhyolites (<5%; [37]) would, if applicable here, lead to reported ages that negligibly over estimate the true ages (~+4 ky per 5% ^{230}Th excess).

Rb–Sr isotope analyses, performed at UCLA, of whole rock samples from domes YA and YG and glass from dome OD were measured by thermal ionization mass spectrometry to confirm that our samples are similar to those previously studied [19,24]. Hand-picked glass shards, visually inspected to be phenocryst-free, from dome OD were used. The Rb–Sr isotope compositions of domes YA and YG were determined on relatively large samples (~50–65 mg), whereas the amount of glass analyzed from dome OD was relatively small (~4 mg) and prepared as a microsample [38].

5. Results

5.1. Nature of zircon in the Bishop Tuff and Glass Mountain rhyolites

Most studied zircons are clear, but may contain inclusions of glass, apatite, and opaque oxides. Except for a relatively small proportion (<5%) of slightly rounded and cloudy crystals in the BT and some subhedral grains in Dome YA, the majority of studied zircons are euhedral. Most analyzed zircons are inferred to represent isolated microphenocrysts. This is based on both the presence of host glass adhering to

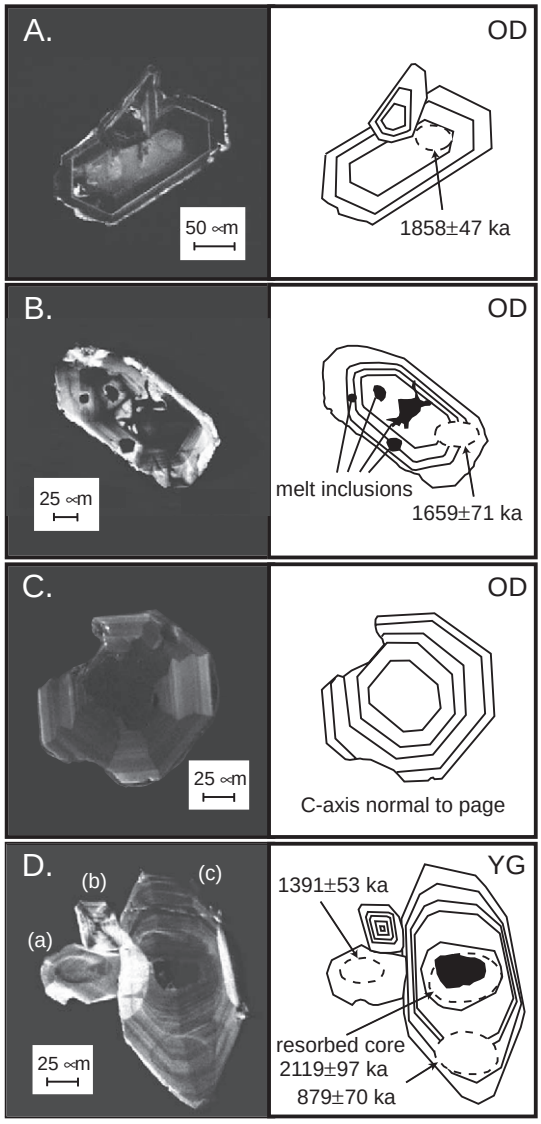

Fig. 2. Cathodoluminescence images and illustrations of representative Long Valley zircon textures (including rare resorbed core) with ion microprobe spots indicated by dashed ellipses: (A) dome OD euhedral grain with bright core, (B) dome OD subhedral grain with dark core, (C) dome OD euhedral grain oriented normal to page to show zoning (not measured for age), and (D) dome YG cluster of euhedral grains that contain old core ages (GMII-r1g1s2 and GMII-rg3s1) as well as relatively young rim growth.

the zircon and the homogenous distribution of zircon in the studied rhyolites. Scarce Mesozoic-aged zircons, as identified by U–Pb analyses, are typically cloudy and subhedral to anhedral. Most Quaternary zircons in the studied Long Valley rhyolites exhibit concentric zoning in cathodoluminescence imaging (Fig. 2). A single zircon contained in Dome YG exhibits a texture consistent with resorption and later magmatic overgrowth.

5.2. Zircon ages and compositions

The weighted mean zircon crystallization ages and associated values for the mean square of the weighted deviates (MSWD) [39,40] of each zircon population are summarized in Table 1; individual ages, Th/U ratios, and U concentrations for zircons analyzed in this study can be found in the Appendices. An MSWD of unity is expected for analytical results that are normally distributed around a single mean value. Some deviation from unity is to be expected statistically and so Table 1 also provides the MSWD values at the upper 95%-confidence interval on a single age distribution at the degrees of freedom appropriate for each rhyolite. Except for the EBT, the MSWD values for the zircon populations exceeds that expected for a single age (see Table 1), suggesting that crystallization of each zircon population was protracted (≥50 ky). In

Table 1
Summary of zircon crystallization ages of Long Valley rhyolites[a]

Sample	Mean age (ka)	Analyses (n)	Grains	MSWD[b]	Eruption age[c]	Mean pre-eruption age (ka)[d] (n, MSWD)	Limits on age range (ka)[e] Min (n, MSWD)	Max (n, MSWD)	Sample location
Glass Mountain Rhyolites									
Dome OD (R00LV63)									37°47.187′ lat.,
interiors	1853 ± 13	24	13	2.8 (1.7)	1686 ± 6	1904 ± 15 (n = 20, 1.3)	1728 ± 43 (n = 4, 0.80)	2010 ± 30 (n = 6, 0.18)	118°48.925′ long.
<2 μm surfaces	1706 ± 35	7	6	1.3 (2.6)					
Dome YG (R00LV62)	933 ± 17	13[f]	7	2.2 (1.9)	900 ± 30	984 ± 22 (n = 10, 1.5)	860 ± 25 (n = 4, 0.15)	1066 ± 39 (n = 4, 1.09)	37°47.138′ lat., 118°47.809′ long.
Dome YA (JS01LV04)	981 ± 18	11	11	2.3 (2.1)	790 ± 20	995 ± 19 (n = 9, 2.2)	889 ± 31 (n = 4, 0.03)	1072 ± 28 (n = 4, 0.94)	37°49.486′ lat., 118°45.718′ long.
Bishop Tuff									
LBT (R99LV51)	811 ± 7	20	14	3.4 (1.8)	760 ± 2	849 ± 10 (n = 13, 1.7)	753 ± 11 (n = 7, 0.44)	901 ± 17 (n = 4, 0.70)	37°52.617′ lat., 119°08.433′ long.
EBT (R99LV58)	841 ± 8	29	29	0.9 (1.6)	760 ± 2	853 ± 9 (n = 21, 0.7)[g]	767 ± 30 (n = 4, 0.10)	917 ± 27 (n = 4, 0.05)	37°27.960′ lat., 118°23.017′ long.
EBT (from [21])	823 ± 14	22	20	0.8 (1.8)	760 ± 2	851 ± 13 (n = 13, 0.2)[g]			localities 16/17 and 24 of [64]

[a] All uncertainties are reported as 1 σ_m (ages > 100 Ma excluded).
[b] Mean Square of the Weighted Deviates (MSWD). Value in parentheses is the highest value expected at the 95% confidence interval for normal scatter associated with a single age population (see text).
[c] Ar/Ar or K–Ar eruption ages.
[d] Model mean pre-eruption age obtained by sequential omission of the youngest ages until remaining population yields an MSWD value consistent with single age, except for EBT (see text).
[e] Minimum and maximum ages obtained by pooling 4 or more of oldest and youngest ages, respectively, until the associated MSWD is just within that expected at the 95% confidence interval for the relevant degrees of freedom (see text).
[f] Data from core of YG grain and second adhering grain (1.4–2.1 Ma) excluded from weighted mean.
[g] Pre-eruption age for EBT estimated from age population exclusive of ages within uncertainty of eruption.

order to provide a better but still conservative estimate for the mean age of "pre-eruption" zircon crystallization, the youngest zircon ages were sequentially excluded until, for each age population, the remaining ages yield an MSWD value that is consistent with a single mean age. For the EBT, the pre-eruption age was estimated by excluding ages within uncertainty of the eruption age. The resulting model mean age of pre-eruption crystallization assumes that the youngest zircons crystallized close to the time of eruption and, in effect, that a single episode of zircon crystallization predated eruption; the former assumption seems justified by the similarity between ages of the youngest zircons and those for eruption. The mean age of pre-eruption crystallization is conservative because not all eruption-aged growth may have been excluded and because spatial averaging with younger growth zones by the ion beam may mean that the true age of the cores are not determined. To bracket the possible span of zircon crystallization, maximum and minimum zircon age estimates were obtained by pooling four or more of the oldest and youngest ages of each rhyolite, respectively, until the scatter of the pooled ages is within that expected at the 95%-confidence interval on a single age population. All uncertainties reported in the paper are 1 standard error (σ_m).

5.2.1. Glass Mountain zircons

Based on maximum and minimum ages calculated from the age distributions, zircon crystallization in dome OD, the youngest known of the older GM rhyolites [41], probably occurred sometime between 2010 ± 30 to 1728 ± 43 ka ($n = 19$ crystals). A weighted mean age for the zircon surfaces is ~150 ky younger than the mean age of their interiors (Table 1) and >250 ky younger than a significant fraction of the zircons (4 of 13). Most zircons from dome OD have high U concentrations of >4000 ppm (Fig. 3). Most zircon growth in dome YG, an obsidian from the younger group, apparently occurred sometime between 1066 ± 39 ka and 860 ± 25 ka ($n = 7$ crystals). The zircon grain (GMIIr1g1) from this dome that contains a resorbed core (Fig. 2D) yielded ages of 2119 ± 97 ka for the resorbed core, 1018 ± 53 after the resorbed core was removed by repolishing, and 879 ± 70 ka close to the rim. Thus the region

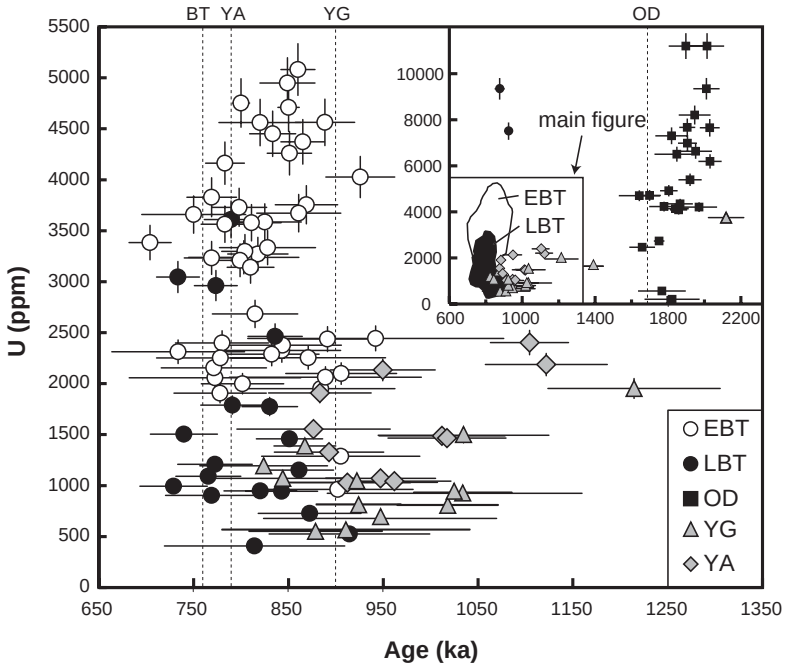

Fig. 3. Ages and U concentrations of zircons from Long Valley rhyolites. In order of decreasing eruption age (indicated by vertical dashed lines), they are: dome OD (black squares), dome YG (shaded triangles), dome YA (shaded diamonds), and the EBT (open circles) and LBT (black circles) (all uncertainties are 1 σ_m).

surrounding the resorbed core probably grew during the same time interval as the other zircons from dome YG. The core of a second grain attached to this one also yields a relatively old, possibly mixed, age of 1391 ± 53 ka. The U concentration of the resorbed core is significantly higher (~3750 ppm) than those of other dome YG zircons (≤2000 ppm). Zircons in dome YA, another member of the younger group of rhyolites, probably have a similar range of ages, from 1072 ± 28 ka to 889 ± 31 ka (n = 11 crystals) with U concentrations that range to slightly higher values (≤2400 ppm). Despite their ~200 ky age spans, the overall distributions of zircon ages in these younger domes exhibit a marked skewedness toward younger ages and most are within ≤100 ky of the youngest zircon age obtained for each rhyolite.

5.2.2. Bishop Tuff zircons

The LBT contains evidence for zircon crystallization from 901 ± 17 to 753 ± 11 ka (n = 14 crystals; Table 1). New ages for EBT zircons (n = 29 crystals) exhibit an identical range, from 916 ± 27 to 767 ± 15 ka. The weighted mean ages of EBT and LBT zircons differ by ~30 ky but mean pre-eruption ages for all samples, including those of [28] are identical at 850 ka. Mesozoic ages obtained on six (five in this study) zircons from the EBT and a single zircon from the LBT are excluded from all weighted mean ages. In general, zircons from the EBT have higher U concentrations (mostly >1800–4500 ppm) than those contained in the LBT (mostly ~100's to <2000 ppm; Fig. 3), as found previously [23]. Uranium concentrations of EBT zircons are also higher than, but those of LBT zircons are similar to, those from the younger GM rhyolites.

5.3. Sr isotopic compositions of GM rhyolites

Rb–Sr isotope data for the studied GM samples are reported in Table 2. $^{87}Sr/^{86}Sr$ ratios for the whole rock samples of YG and YA and a glass from dome OD are ~40 and ~100 ppm lower, and 200 ppm higher, respectively, than previously reported [24]. Because of correlated differences in $^{87}Rb/^{86}Sr$, the data still fall along the isochrons [19,24] that define their respective groups (see Section 2). The differences pale in comparison to the extreme variability of $^{87}Rb/^{86}Sr$–$^{87}Sr/^{86}Sr$ isotopes measured in GM rhyolites, especially between crystals and glass in individual samples (e.g., $^{87}Sr/^{86}Sr$ ~0.706 versus >0.9; [24]), and probably reflect natural heterogeneity and/or differences in the ratios of glass to incidental crystals between samples.

6. Magmachronologies for Glass Mountain and Bishop Tuff rhyolites

In this section, we summarize existing evidence for the timing of differentiation and crystallization in the GM and BT rhyolites and compare them to the zircon results. Most of the existing "magmachronology" for the GM and BT rhyolites is based on mineral model ages (i.e., mineral–glass pairs) and there is some latitude in the validity of these ages. First, the relevance of a model age for melt evolution depends

Table 2
Rb–Sr isotope data for selected Glass Mountain rhyolite obsidians

Sample	Material	Dome	Crystal %	Rb (ppm)	Sr (ppm)	$^{87}Rb/^{86}Sr$[a]	$^{87}Sr/^{86}Sr$[a]	2 σ_m
R00LV63	glass	OD	†	252.0	1.81	403.9	0.717486	± 11
R00LV62	whole-rock	YG	6–7	145.8	1.98	212.9	0.708869	± 14
JS01LV04	whole-rock	YA	<2	150.0	2.13	204.0	0.709386	± 14

† Visible crystals excluded; disseminated impurities unavoidable.

[a] Ratios reflect total process blank corrections and normalization: blank for Sr was ~0.5 ng with a weighted mean $^{87}Sr/^{86}Sr$ ratio of 0.7112 ± 3 (95% confidence level, n = 9). Based on blank measurements, corrections of 92, 93, and 350 ppm for YG, YA, and OD were applied, respectively to $^{87}Sr/^{86}Sr$. All $^{87}Sr/^{86}Sr$ ratios normalized so that $^{84}Sr/^{86}Sr$ = 0.1194 and then corrected by +29 ppm for direct comparison to previous studies: weighted average $^{87}Sr/^{86}Sr$ ratio for NBS987 measured for this study was 0.710230 ± 16 (2 σ_m, n = 20) versus $^{87}Sr/^{86}Sr$ = 0.710259 [20]. Blank corrections were also applied to Rb and Sr abundances. Reported uncertainties in $^{87}Sr/^{86}Sr$ ratios are in-run precision.

on a mineral's affinity to its host. This dependence is particularly acute in the case of the Rb–Sr ages since these ages are largely determined by their respective glass compositions. Second, the model ages may be affected by compositional heterogeneities in the crystals and diffusive re-equilibration. At least for the Rb–Sr feldspar ages that comprise the majority of these ages, diffusion does not appear to be appreciable at the relevant magmatic conditions [42] but this also means that the model ages will be biased towards the timing of crystallization of the feldspar crystals' more Sr-rich cores.

Zircons are retentive of radiogenic Pb even at supersolidus conditions (e.g., ~700–900 °C) [43] and their U–Pb ages are relatively free of uncertainties in their common Pb isotope composition. Therefore, ages obtained by U–Pb analyses record the timing of zircon crystallization which, in turn, is expected to accompany crystallization of the major mineral phases in rhyolites [21,44]. Magma storage and even progressive fractionation of rhyolites would not necessarily erase an earlier zircon crystallization record [28,45]. Thus, the U–Pb ages of the zircon can be used to corroborate the validity of the Sr model ages and, by extrapolation from these and the chemical characteristics of the zircons, the timing of differentiation.

6.1. Sr, Nd, and Ar isotope considerations for the evolution of Glass Mountain and Bishop Tuff rhyolites

A remarkable feature of glass and whole rock samples from the GM domes is that their Rb–Sr isotopic compositions define trends that may reflect four distinct regional episodes of mineral–melt segregation [18,24] (cf. [46,47]): two at ~2.05 and ~1.89 Ma for the older domes and two at ~1.15 and ~1.09 Ma for the younger domes. The oldest Sr mineral model ages are within tens of ky of those obtained for differentiation [18,19]. Eruptions followed the apparent timing of Rb–Sr fractionation by a few ky to ~360 ky. Affinities between GM crystals and their hosts are supported by the similarity of Nd and Pb isotope ratios and Sr and Rb abundances found among crystals contained within individual rhyolites, and by the fact that Rb–Sr isochrons appear to have been protected from disruption by crystal–liquid separation for 10's to 100's of ky [18]. Those few feldspar model ages that are both older than apparent differentiation and younger than eruption [18] may be indicative of crystal exchange between melts [48], magma mingling and/or assimilation, or other open system processes.

Rb–Sr isotope characteristics of the BT are more scattered than those for GM rhyolites [13,15,19], but most glasses could have evolved from a common reservoir at ~1 Ma (see evolution diagram in Fig. 4) or even before if differentiation was less punctuated and

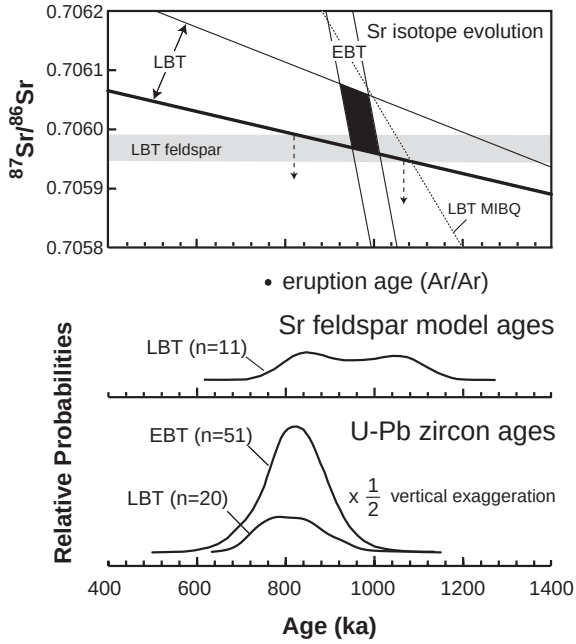

Fig. 4. Summary of isotopic constraints on the differentiation and crystallization history of the Bishop Tuff. *Upper portion of figure*: Sr isotope evolution diagram. Evolution lines bound Sr isotope trajectories for feldspars (horizontal shaded region) and host rhyolite glasses (solid lines); the bold LBT evolution curve indicates the host glass for the Sr model feldspar ages shown in the lower part of this figure. An evolution line is given for the sole LBT MIBQ (dotted line). Data of [15,19]. Notably a majority of EBT and LBT glasses intersect at ~1 Ma (black fill), just prior to crystallization of the oldest zircon. Exceptions (not shown) include EBT glass sample BT-6 [15] that gives a model age of ~2.2 Ma, LBT glass sample BT-24 that yields no meaningful age and is from an outcrop that [13] suggest may have experienced post-eruptive alteration, and EBT MIBQ (see text). Whole rock data from [13] are not shown because they yield relatively few potentially meaningful ages and are therefore ambiguous. *Lower portion of figure*: Relative probability curves of LBT Sr feldspar model ages [19] and BT U–Pb zircon ages (this study). The range in LBT model feldspar ages is probably not real since they have analytically identical isotopic compositions but the mean age appears to be somewhat older than our zircon ages. EBT model feldspar (not shown) exhibit a range from −1326 to 948 ka and are therefore ambiguous ([19]; see text for details).

more progressive (cf. [15]). Of those glasses that scatter from this apparent BT Rb–Sr isochron, one yields a GM-like model age (~2.2 Ma) but it may be contaminated [15]. LBT feldspars are like their host melts in their initial Nd isotope signatures and yield Sr model ages that are similarly permissible of crystallization up to ~300 ky before eruption [19,20] (Fig. 4). On the other hand, many EBT feldspars could not have grown from their hosts because, despite having lower Rb/Sr, they have more radiogenic Sr isotope signatures than the EBT at the time of eruption [19]. In addition, to the extent that they are known, most feldspars are distinct in their Nd isotope signatures from their host pumice. Many of the radiogenic feldspars are characterized by anomalously low Sr contents and a subset of sanidines exhibit rimward enrichments in compatible elements (e.g., Sr and Ba) (data of [19,49]).

Single BT quartz crystals are observed to be heterogeneous in both their oxygen isotope signatures [17] and in the Rb/Sr ratios of melt inclusions they host (~200–600, [26]) and therefore could have grown from a range of melt compositions. These melt inclusion-bearing quartz (MIBQ) have Nd isotopic compositions like those of their hosts and, for LBT MIBQ, Sr isotopic compositions that could reflect ~300 ky of aging [13,20], especially when compared to the isotopic compositions of coexisting feldspars. Those for EBT MIBQ range to significantly more radiogenic Sr isotope values than their host which, if resulting from in situ decay, could indicate that they are derived from residual GM-aged (>1.9 Ma) material [15,19,20]. Thus, both EBT MIBQ and some EBT feldspars have Sr isotopic signatures that are too radiogenic for growth from the BT magma in a ≤300 ky interval before eruption but only the radiogenic MIBQ could be explained by derivation from earlier episodes of Long Valley activity.

Argon isotopic compositions of MIBQ [16] from the EBT indicate apparent ages (1.7–2.3 Ma) similar to those of the GM rhyolites. Ages for the LBT MIBQ (1.4–4.6 Ma) overlap and extend this range, and are thus at variance with ≤1.1 Ma Sr model ages for the same minerals. It is uncertain how melt inclusions in quartz could have remained closed to Ar loss and/or gain at magmatic conditions (cf. [50,51]) and apparent ages significantly older than GM activity, especially for the LBT MIBQ, suggest that the MIBQ incorporated excess ^{40}Ar [50,51]. In light of this, the Ar isotope data of MIBQ as a chronologic constraint will not be considered further in this paper.

6.2. Relationship of U–Pb zircon crystallization ages to other magmachronologies for the Glass Mountain and Bishop Tuff rhyolites

The range of zircon ages for each of the studied rhyolites indicates time periods where compositional and thermal conditions were appropriate for zircon growth and thus provide important absolute bench marks for reconstructing the history of silicic magmatism (e.g., [52,53]). Here we evaluate foregoing estimates for the timing of differentiation, crystallization, and eruption in light of our zircon ages.

Dome OD is the youngest known "older group" GM rhyolite based on its Ar/Ar eruption age of 1.686 ± 0.006 Ma (1 σ) from concordant sanidine step-heating and total fusion isochron ages [18]. The concordance of the youngest of the 31 zircon ages for this dome, and in particular the <2 μm surface measurements, with the Ar/Ar ages appears to corroborate this eruption age estimate (Fig. 5). The 6 oldest zircon ages for dome OD are, on the other hand, comparable to the ~1.97 to ~2.04 Ma Sr model ages [18] for major minerals as well as for the accessory phases with which zircon is observed to be intergrown. These same 8 ages could represent a single age population (Table 1) that is within error of the ~2.05 Ma OGM differentiation isochron that includes dome OD (Fig. 5), and thus support the conclusions of [18] from Sr isotope considerations that crystals contained within dome OD could have formed close to the time of differentiation. Ages for several zircon interiors fall between these two extremes. Although this age spread could reflect, in part, spatial averaging by the ion beam of early and late growth zones, zircon *interiors* that range to as young as the time of eruption (~1.7 Ma) suggest instead the zircon growth may have been more continuous. Overall, the distribution of zircon ages overlaps and extends the age span inferred from the Rb–Sr isotope data. Moreover, it suggests that nucleation and crystallization was protracted rather than punctuated at ~2 Ma as implied by the Sr mineral model ages [18].

Most zircon ages in dome YG, a rhyolite from the "inner" suite of the two younger GM groups, are younger than ~1.0 Ma and more than half of the 7

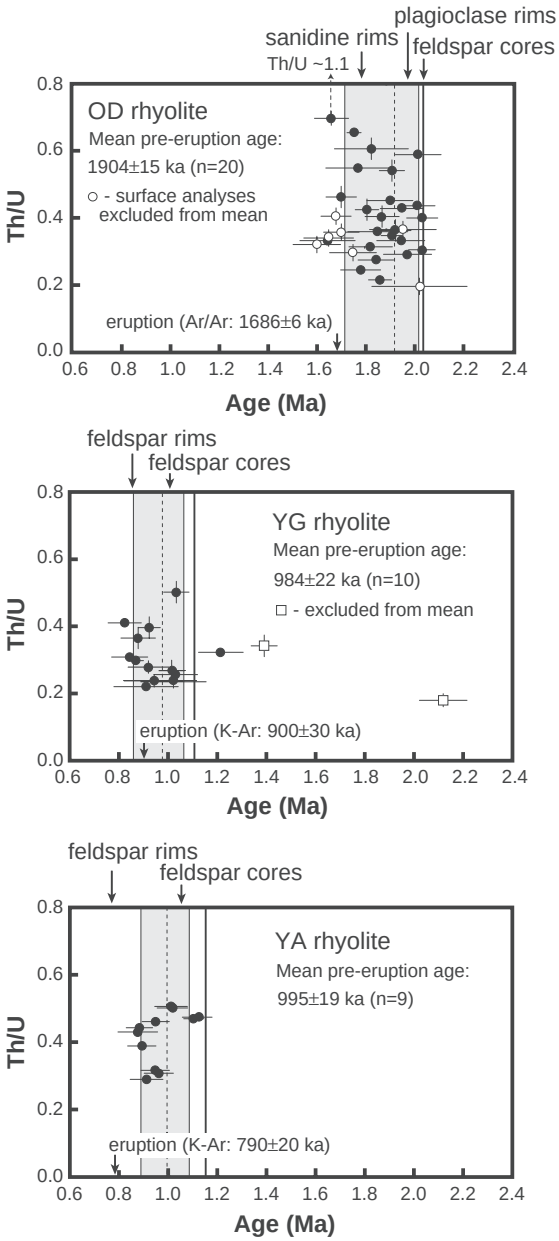

Fig. 5. Comparison of the distribution of U–Pb zircon crystallization ages to reported K–Ar and Ar/Ar eruption ages, feldspar Sr model ages, and regional Rb–Sr isochron ages (bold vertical line) for studied GM rhyolites. Circles indicate individual zircon measurements, dashed vertical lines show the mean pre-eruption ages, and shaded vertical bands show possible span of zircon crystallization based on pooling older and younger ages, respectively (Table 1), for each rhyolite (see text for details). For each mean age, n gives the number of analyses. All uncertainties are 1 σ.

zircons analyzed could have grown at ~0.8–0.9 Ma. This age range corresponds to that bracketed by feldspar Sr model core (~0.99–1.01 Ma) and rim (0.84–0.87 Ma) ages [19], as well as a K–Ar eruption age of 0.90 ± 0.03 Ma (1 σ) from host glass [30]. The MSWD for the YG zircons that fall in this age range is in excess of the value expected from analytical scatter for a single age (Table 1). Collectively, therefore, the data suggest that feldspar and zircon crystals in the dome YG rhyolite grew between ~1.0 Ma and eruption at ~0.84 Ma (Fig. 5). Protracted magma residence is supported by the zircon model pre-eruption age of 984 ± 22 ($n = 10$). Only two ages (~1.4 and ~2.1 Ma) on a zircon glomerocryst (Fig. 3D) are significantly older than the ~1.1 Ma timing of apparent differentiation of YG [19]. This glomerocryst could have been inherited from older GM (1.7–2.1 Ma)-related rhyolitic magmas or solidified intrusive bodies if the 1.4 Ma "age" reflects simultaneous sampling by the ion microprobe beam of portions of a hybrid grain that grew during both the older and younger episodes of GM magmatism.

As with dome YG, the MSWD value obtained for the 11 analyzed zircons from dome YA, a member of the "outer" group of younger GM rhyolites, is in excess of the value expected from analytical scatter for a single age and may reflect a range of crystallization ages; protracted magma residence is supported by the zircon model pre-eruption age of 995 ± 19 ($n = 9$) (Table 1). The oldest zircon ages in YA (~1.1 Ma) are within error of the composite Sr model age of YA plagioclase cores (~1.1 Ma), as well as the regional whole-rock glass isochron age of ~1.15 Ma [19]. The youngest zircons are not, however, as young as a 0.79 ± 0.02 Ma (1 σ) K–Ar eruption age obtained for dome YA glass [30] (Fig. 5). By analogy to the presence of eruption-aged zircons in other studied Long Valley rhyolites, the youngest U–Pb zircon ages could indicate that eruption occurred closer to ~0.9 Ma, rather than ~0.8 Ma. In apparent contradiction to this interpretation are the ~0.78 Ma composite feldspar rim Sr model ages. It is possible that near-eruption age zircon growth was absent, as has been observed in similar studies elsewhere (cf. [28,45]), or not detected (no surface ages were measured for either younger GM domes). Alternately, these younger feldspar ages could be explained by crystallization from magma with higher

$^{87}Sr/^{86}Sr$ than the one in which they were erupted. For example, the feldspar rims could be up to ~150 ky older if they grew from a high Rb/Sr member of the same ("outer isochronous") rhyolite group. If the YA plagioclase cores also grew from that magma, their model ages would be ~50 ky closer to the regional isochron age but still within error of the oldest zircon ages. These two interpretations, minimal near-eruption zircon growth versus late-stage magma mixing, might be distinguished by higher resolution Ar isotope dating.

At ~850 ka, pre-eruption mean zircon ages for all BT samples are about 90 ky older than an Ar/Ar sanidine eruption age of 760 ± 2 ka [16]. This mean pre-eruption age represents a robust minimum for the oldest crystallization in the BT with the maximum no more than ~200 ky prior to eruption (cf. [21]). The Sr isotope diversity of most of the BT glasses could have developed over nearly the same time interval (Fig. 4) even without the possible effects of assimilation [54]. The distribution of LBT feldspar model ages appears similar to but slightly broader than the span of measured zircon ages but the feldspars ages are within analytical uncertainty of each other and (excluding rim data) give a weighted mean age of 987 ± 35 ka only slightly older than the oldest zircons. Glasses in EBT MIBQ are, on the other hand, too radiogenic to have been trapped from their host melts in the <300 ky of zircon crystallization (Fig. 6). Although this *could* be taken to indicate that the MIBQ are older than the zircon, it is difficult to imagine a magmatic scenario in which zircon is selectively lost [28,45]. The anomalously radiogenic EBT feldspars, which constitute an

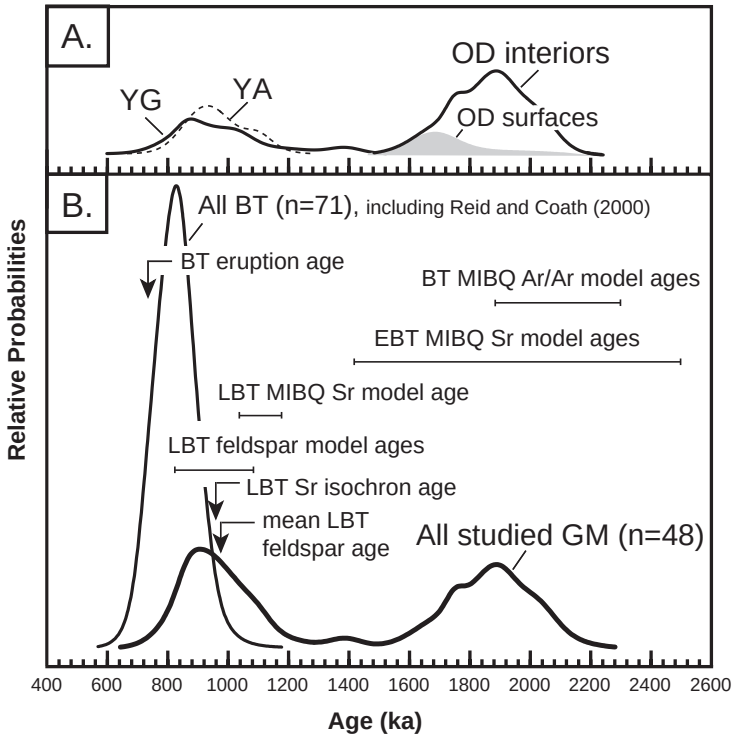

Fig. 6. Cumulative probability distributions of GM and BT U–Pb zircon ages shown along with other estimates for crystallization and eruption of the BT: (A) Zircon ages for GM domes OD, YG, and YA (<2 μm deep surface analyses for dome OD shown by filled region). (B) Zircon ages for BT (includes data of [21]). Also shown is the zircon age population distribution for all studied GM rhyolites, reference to which demonstrates the relative lack of GM-aged zircon in the BT. Eruption and MIBQ Ar/Ar ages are from [16], MIBQ Sr model ages are from [20], and LBT feldspar model ages are from [19] based on an initial ratio of 0.706. A single 958 ± 10 ka Rb–Sr isochron with a $^{87}Sr/^{86}Sr_i = 0.70638$ can be fit to the "intermediate" and late MIBQ and associated feldspar data of [20]. The weighted mean age of LBT feldspar of [19] (excluding rim data) is 987 ± 35 ka.

appreciable portion of the feldspars analyzed to date, suggest an alternate scenario. These feldspars provide evidence for isotopic and chemical heterogeneity in the nascent BT magma chamber. Accordingly, both the radiogenic quartz and feldspar could have crystallized contemporaneously with the zircons from a more radiogenic portion of the magma chamber. An important inference that would apply is that a significant fraction of the minerals contained in the EBT would not have crystallized solely from their host melts.

7. Rhyolite evolution as revealed by zircon crystallization ages

7.1. Relative timing of differentiation and crystallization

Our ion microprobe analyses of age domains within individual zircons reveal a record of the relationship between differentiation and crystallization that is similar to, but more detailed than, other recent studies [55,56]. The concordance between the oldest zircon ages in the studied GM rhyolites and their respective regional Sr isochrons apparently reflects the onset of crystal growth soon after melt differentiation (cf. [45,56]). Subtle differences between the range of zircon and feldspar Sr model ages could, in part, reflect differences in the scale of the two types of analyses (i.e., spots within individual zircons versus bulk composites and single feldspar grains). Additionally, the broader range of zircon crystallization ages (e.g., $\geq$200 ky for dome OD; Table 1) than those of feldspar Sr model ages (~10's ky) could, in part, reflect selective analysis of only the largest (and presumably oldest) feldspars (cf. [18]). The reproducibility of the zircon ages for a given rhyolite suggests that even though the ion microprobe spots may sample multiple growth zones, the cores are not vastly older than these ages. Only the zircon glomerocryst contained in YG provides evidence for carry-over of material from one (older GM) to another (younger GM) rhyolite. Such intergrowth of zircon suggests that the glomerocryst originates from partial assimilation of preexisting older GM-aged intrusive bodies (cf. [7]). As detailed below, the crystal record of the BT also appears populated by zircons that formed after differentiation rather than, for example, being entrained during expulsion of melt from a mushy reservoir (cf. [3,4]) or otherwise being the survivors of stochastic crystal–liquid separation.

7.2. Zoning of the caldera-related magma system

The BT changed in composition during the course of its eruption [22]. Gas saturation pressure constraints [57], which correlate with a compositional shift from more to less evolved rhyolite during the eruption, are consistent with progressive withdrawal of magma from a vertically zoned reservoir [23]. Affinities of mineral assemblages to host pumice compositions indicate that the compositional diversification of the system largely preceded crystallization of the mineral assemblage present [13,15,18,23,58]. Nonetheless, variations among compatible and incompatible trace element concentrations in MIBQ form separate differentiation trends for the EBT and LBT (cf. [26,44]). This dichotomy is corroborated by the distinct U abundances we measured in EBT and LBT zircon populations (Fig. 3) that likely reflects crystallization from compositionally distinct melts [23]. The greater scatter in the ages of the LBT zircons compared to those of the EBT zircons (compare MSWDs in Table 1) may, judging by the similarity between LBT and EBT pre-eruption crystallization ages, reflect a greater proportion of near-eruption aged crystallization in the case of the LBT.

Many BT feldspars and MIBQ are too radiogenic to have crystallized from Long Valley magmas and hence cannot be explained even by models of progressive and protracted development of compositional zoning. We infer that the radiogenic feldspars and MIBQ in the BT co-crystallized from melts that are more radiogenic than the hosts in which they are found. The anomalously low Sr contents of many of the unusually radiogenic feldspars also means that the melts from which these feldspars crystallized could have had a negligible influence on the final isotopic composition of the BT. Rimward increases in compatible elements (e.g., Sr and Ba) (data of [19,25,26,49]) in a subset of EBT and LBT sanidines and heterogeneous populations of inclusions in a subset of the MIBQ which could represent "some irregular (open-

system) changes" [59], e.g., localized magma mingling [26], also provide evidence of open system processes in the BT. Some but not all of these features can be explained by injection of less evolved rhyolite into the LBT [25,26,59,60].

The identical age ranges of the respective EBT and LBT zircon populations are remarkable since they imply that more and less evolved portions of compositionally zoned rhyolites can develop simultaneously rather than sequentially. Zonation could have been produced by sidewall fractional crystallization [58] only if it is sufficiently rapid (<10's ky). The compositional differences could alternately and/or additionally be explained by accumulation of distinct melts that separated virtually simultaneously from a compositionally heterogeneous crystal mush (i.e., distinct interstitial melt domains that form from different degrees of in situ crystallization [61]). In either case, differences between the EBT and LBT apparently originated largely by the rapid (10's ky) accumulation of broadly cogenetic melts rather than progressive and protracted (>1 my) compositional zonation [15].

7.3. Intermittent differentiation and storage of rhyolite

The studied rhyolites contain zircon populations that provide "finger-prints" of magmas with distinctive crystal records (Fig. 6). Evolved, zircon-saturated liquids were at least periodically present within the Long Valley magmatic system between ~2.0 to ~1.7 Ma (dome OD) and ~1.1 to ~0.76 Ma (domes YG and YA, and the BT). This bimodal age distribution contrasts with the continuous zircon age distribution that might be expected if a largely molten silicic magma reservoir was persistently present. The absence of zircons of intermediate ages (~1.7 to ~1.2 Ma) could reflect a compositional reversal towards a more mafic, zircon-undersaturated resident magma. In this case, the lack of contemporaneous volcanic activity [14] would require that the magmas never erupted or were destroyed during caldera formation or otherwise buried. Rather than a shift to more mafic compositions, this gap in the GM zircon crystallization record could alternately reflect a diminished magmatic influx from the mantle and partial to complete solidification of resident magmas. Whichever possibility applies, the two suites of GM rhyolites likely require distinct episodes of differentiation.

The age populations of the younger GM and the BT zircons suggest that there was some overlap (10's ky) in the time period of crustal residence between their magma reservoirs. Mean zircon ages for domes YA and YG are ~100 to ~150 ky older, respectively, than that for the BT, even when the oldest, inherited YG cores are excluded. These differences are only partially explained if, as suggested by their youngest zircon ages, both domes YG and YA erupted ≥100 ky before the BT. Even so, the >1 Ma zircons of younger GM are not observed in the BT zircon age population (Fig. 6). Both YGM and BT rhyolitic magmas are expected to be saturated with zircon at the temperatures (740–775 °C) [14,23,27] delimited from their phenocryst assemblages and host glass and so if phenocrysts were inherited, as previously inferred, we should find evidence of GM-aged zircon inheritance as well. These age constraints, coupled with the distinct ranges of younger GM and BT crystal compositions (e.g., U concentrations in zircon, this study and [23], and Sr concentrations in feldspar [19]), support evidence from differences in whole rock compositions (e.g., LREE enrichment of the LBT [14]) that the evolutionary history for the BT rhyolites was separate from that for the younger GM rhyolites. If magma associated with or residual to the younger GM rhyolites was incorporated by the BT, it was evidently very minor or zircon in the BT reservoir was unstable.

Collectively, the various groups of Long Valley rhyolites appear to be the product of periodic, rapid (no more than ~50 ky before zircon nucleation) differentiation rather than tapping a long-lived, integrated *rhyolitic* magma body. Minimum production rates of $\sim 4 \times 10^{-3}$ to $\sim 1 \times 10^{-2}$ km^3/yr for the BT based on our zircon age constraints (~150 to 70 ky) [62] are approximately an order of magnitude greater than those obtained previously (0.7×10^{-3} to 2.7×10^{-3} km^3/y calculated from [15]) and in the upper limit are comparable to the time-integrated production of basaltic magma [2]. Rhyolites may differentiate relatively rapidly from a crystal-rich, "mushy" magma column by gravitational collapse (e.g., [4]) and/or gas-driven filter pressing [3]. Alternatively, the source could be underplated magmas, and differentiation could have occurred by

partial melting (e.g., [10]). Once differentiated, the liquids may be stored as co-existing, but separate magmas (cf. [63]), possibly within a non-convecting mush. Significantly, despite their small size, it appears that zircons from the mushy or restitic source are largely not entrained in derivative liquids, because zircon ages postdate the apparent timing of Rb/Sr fractionation, and therefore bulk chemical fractionation.

8. The buildup to caldera formation in the Long Valley magmatic system

Population studies of the datable crystal record contained in Long Valley rhyolites provide a powerful tool for reconstructing the complex history of the magma system that existed beneath the present Long Valley region. Differentiation occurred rapidly (≤10's ky) for the small-volume (<1 km^3) GM rhyolites that erupted intermittently before the major caldera-forming event, based on the concordance of the oldest zircon growth and Rb–Sr fractionation. Crystallization may have been prolonged (≥200 ky). The BT rhyolite differentiated while the younger GM rhyolites were being stored but was isolated from them, possibly as a separate magma body in a non-convecting mushy magma reservoir. The BT acquired its compositional zoning before zircon crystallization, indicating either rapid (≤50 ky) internal differentiation compared to zircon growth or virtually synchronous segregation from distinct regions of crystal mush. We conclude that groups of rhyolites at Long Valley, California, are the product of transient melts that represent discrete episodes of silicic magmagenesis within a >1 my period.

Acknowledgments

We thank C. Bacon and I. Fletcher for their helpful reviews. We also thank A. Schmitt and J. Vazquez for their insightful reviews of an early version of the manuscript. Funding was provided by NSF grant EAR003601 to MRR. The UCLA ion microprobe is partially supported by a grant from the NSF Instrumentation and Facilities Program.

Appendix A. Results of U/Th/Pb ion microprobe analyses of zircon from selected Long Valley rhyolites

Spot number	$^{206}Pb/^{238}U$ ($\times 10^4$)[a]	χ[b]	Age (ka)[c]	σ_m	Th/U	U (ppm)[d]
Glass Mountain Dome OD (R00LV63)[e]						
Interior spot analyses						
GMI-r1g1s2	5.71	0.52	2029	54	0.30	7650
GMI-r1g3s1	2.82	0.85	1643	113	0.33	4701
GMI-r2g1s1	3.24	0.82	1820	89	0.31	7302
GMI-r2g1s1pol	3.28	0.86	1921	64	0.36	5393
GMI-r2g2s1	2.76	0.99	1858	47	0.22	4088
GMI-r2g2s2	2.74	0.97	1804	48	0.42	4917
GMI-r2g2s3	3.04	0.89	1841	73	0.27	4138
GMI-r2g2s1rim	3.05	0.92	1907	52	0.54	6982
GMI-r2g2s2rim	3.18	0.90	1946	87	0.43	8204
GMI-r2g3s1	3.24	0.93	2031	64	0.40	6191
GMI-r2g3s2	3.00	0.92	1867	70	0.40	4347
GMI-r2g5s1	4.46	0.65	1971	99	0.29	4205
GMI-r2g5s1pol	2.58	0.97	1699	62	0.46	4712
GMI-r3g1s1	2.85	0.91	1779	82	0.25	4229
GMI-r3g2s1	3.14	0.95	2011	72	0.44	9346
GMI-r5g1s1	2.83	0.99	1906	44	0.35	7667
GMI-r5g1s2	3.25	0.92	2014	94	0.59	11,199
GMI-r5g1s4rim	3.09	0.90	1898	95	0.45	11,196
GMI-r5g1s5rim	3.35	0.85	1943	98	0.33	6632
GMI-r5g5s1	3.47	0.78	1823	151	0.61	204
GMI-r5g6s1	3.64	0.75	1849	123	0.36	6504
GMI-r7g4s1	2.60	0.99	1751	29	0.65	2736
GMI-r7g4s4rim	4.20	0.62	1767	131	0.55	567
GMI-r7g4s1	2.64	0.93	1659	71	1.12	2464
<2 μm surface analyses						
GMII-r1g1s1	2.89	0.83	1648	102	0.34	4013
GMII-r1g2s1	3.23	0.77	1700	73	0.36	6717
GMII-r1g6s1	3.23	0.76	1678	62	0.41	5110
GMII-r1g7s1	12.45	0.19	1599	97	0.32	3987
GMII-r1g10s2	3.51	0.85	2020	195	0.20	1168
GMII-r2g2s1	9.50	0.30	1952	137	0.37	6635
GMII-r2g5s1	3.03	0.84	1747	96	0.30	247

[a] Raw data.
[b] Fraction of radiogenic ^{206}Pb based on common $^{207}Pb/^{206}Pb$ correction.
[c] Ages corrected for initial ^{206}Pb and ^{238}U-series disequilibrium (see text for details).
[d] U concentrations are ~5% (1 σ) based on comparison to measurement of zircon standard 91500.
[e] Sample nomenclature after [30] and [33] for Glass Mountain domes and the Bishop Tuff, respectively. Analyses are identified by row (r#), grain (g#), spot (s#), near rim location ("rim"), and sessions in which an additional ~5–10 μm was removed by re-polishing ("pol").

Appendix B. Results of U/Th/Pb ion microprobe analyses of zircon from selected Long Valley rhyolites

Spot number	$^{206}Pb/^{238}U$ ($\times 10^4$)[a]	χ[b]	Age (ka)[c]	σ_m	Th/U	U (ppm)[d]
Glass Mountain Dome YA (JS01LV04)[e]						
GMVII-r2g1s1	1.40	0.87	874	81	0.49	1555
GMVII-r2g5s1	1.69	0.84	1009	66	0.58	1488
GMVII-r3g2s1	1.59	0.90	1015	62	0.58	1465
GMVII-r3g4s1	1.60	0.77	891	58	0.45	1328
GMVII-r4g1s1	1.70	0.94	1119	64	0.55	2188
GMVII-r4g2s1	1.45	0.91	946	58	0.36	1072
GMVII-r5g2s1	1.47	0.91	960	60	0.35	1043
GMVII-r5g4s1	1.44	0.87	911	67	0.33	1029
GMVII-r5g5s1	1.75	0.90	1102	41	0.54	2403
GMVII-r5g6s1	1.49	0.89	947	55	0.53	2135
GMVII-r5g7s1	1.41	0.87	881	54	0.51	1909
Glass Mountain Dome YG (R00LV62)[e]						
GMII-r1g1s1rim	1.32	0.92	879	70	0.37	551
GMII-r1g1s2	3.78	0.83	2119	97	0.18	3753
GMII-r1g1s2pol	1.54	0.92	1018	53	0.27	807
GMII-r1g2s1	3.39	0.37	911	131	0.22	566
GMII-r1g3s1	1.81	0.71	923	84	0.28	1025
GMII-r1g3s1pol	2.22	0.90	1391	53	0.34	1642
GMII-r1g3s2	1.61	0.70	824	67	0.41	1193
GMII-r1g4s1	2.57	0.51	947	123	0.24	672
GMII-r1g4s1pol	3.33	0.52	1215	91	0.32	1952
GMII-r1g5s1	2.10	0.69	1035	90	0.26	1487
GMII-r2g1s1	2.68	0.53	1025	134	0.24	918
GMII-r2g1s1pol(x2)	1.52	0.96	1034	52	0.50	929
GMII-r2g1s1pol(x3)	1.26	0.95	867	33	0.30	1389
GMII-r2g1s2polrim	1.39	0.92	924	45	0.40	813
GMII-r2g2s1	2.67	0.43	844	73	0.31	1072

[a] Raw data.
[b] Fraction of radiogenic ^{206} Pb based on common ^{207} Pb/^{206} Pb correction.
[c] Ages corrected for initial ^{206} Pb and ^{238} U-series disequilibrium (see text for details).
[d] U concentrations are ~5% (1 σ) based on comparison to measurement of zircon standard 91 500.
[e] Sample nomenclature after [30] and [33] for Glass Mountain domes and the Bishop Tuff, respectively. Analyses are identified by row (r#), grain (g#), spot (s#), near rim location ("rim"), and sessions in which an additional ~5–10 μm was removed by re-polishing ("pol").

Appendix C. Results of U/Th/Pb ion microprobe analyses of zircon from selected Long Valley rhyolites

Spot number	$^{206}Pb/^{238}U$ ($\times 10^4$)[a]	χ[b]	Age (ka)[c]	σ_m	Th/U	U (ppm)[d]
"*Late*" *Bishop Tuff Ig2NW (R99LV51)*[e]						
LBTIV-r2g1s1	1.33	0.90	872	54	0.38	727
LBTIV-r2g2s1	1.18	0.96	820	38	0.76	947
LBTIV-r2g2s2	1.20	0.97	843	38	0.76	945
LBTIV-r2g3s1	1.20	0.95	830	29	0.42	1775
LBTIV-r2g4s1	1.23	0.96	861	36	0.31	1152
LBTIV-r2g4s2rim	1.21	0.94	836	29	0.44	2464
LBTIV-r3g2s1	2.68	0.41	814	95	0.44	408
LBTIV-r3g2s2	2.22	0.57	914	85	0.60	526
LBTIV-r3g3s1	1.22	0.96	851	35	0.45	1459
LBTIV-r3g4s1	1.14	0.91	772	39	0.38	1208
LBTIV-r3g5s1	1.04	0.96	740	35	0.36	1504
LBTIV-r4g1s1	1.24	0.84	769	49	0.46	903
LBTIV-r4g2s1	1.13	0.95	791	33	0.41	1790
LBTIV-r5g1s1	1.34	0.97	926	25	1.01	7513
LBTIV-r5g1s2rim	1.03	0.96	733	23	0.52	3046
LBTIV-r5g2s2	1.05	0.92	729	36	0.36	994
LBTIV-r5g2srim	1.06	0.97	765	34	0.31	1092
LBTIV-r5g3s1	1.18	0.91	789	28	0.63	3611
LBTIV-r5g4s1rim	1.09	0.96	773	23	0.48	2962
LBTIV-r5g4s2	1.24	0.98	877	28	0.87	9349
Xenocryst						
LBTIV-r3g1s1	526.56	0.59	197×10^3	14×10^3	0.44	306

[a] Raw data.
[b] Fraction of radiogenic ^{206} Pb based on common ^{207} Pb/^{206} Pb correction.
[c] Ages corrected for initial ^{206} Pb and ^{238} U-series disequilibrium (see text for details).
[d] U concentrations are ~5% (1 σ) based on comparison to measurement of zircon standard 91 500.
[e] Sample nomenclature after [30] and [33] for Glass Mountain domes and the Bishop Tuff, respectively. Analyses are identified by row (r#), grain (g#), spot (s#), near rim location ("rim"), and sessions in which an additional ~5–10 μm was removed by re-polishing ("pol").

Appendix D. Results of U/Th/Pb ion microprobe analyses of zircon from selected Long Valley rhyolites

Spot number	$^{206}Pb/^{238}U$ ($\times 10^4$)[a]	χ[b]	Age (ka)[c]	σ_m	Th/U	U (ppm)[d]
"*Early*" *Bishop Tuff Ig1Eb (R99LV58)*[e]						
EBT-r1g1s1	1.59	0.67	778	49	0.42	1907
EBT-r1g3s1	1.48	0.82	869	33	0.67	3754
EBT-r1g4s1	1.48	0.84	889	31	0.71	4563
EBT-r1g5s1	1.46	0.77	815	45	0.60	2684
EBT-r1g7s1	1.56	0.83	926	36	0.63	4027
EBT-r2g1s1	1.35	0.81	802	43	0.35	1999
EBT-r2g2s1	1.95	0.63	885	78	0.52	1952
EBT-r2g3s1	1.54	0.80	892	44	0.48	2437
EBT-r2g5s1	1.62	0.65	772	56	0.38	2154
EBT-r2g6s1	1.78	0.65	843	62	0.44	2326
EBT-r2g7s1	1.45	0.82	861	44	0.39	3673
EBT-r2g8s1	1.65	0.76	906	58	0.33	2099
EBT-r2g9s1	2.40	0.51	889	101	0.45	2062
EBT-r2g10s1	1.90	0.52	734	70	0.38	2313
EBT-r2g11s1	2.16	0.49	773	91	0.43	2058
EBT-r3g1s1	1.26	0.91	834	24	0.62	4452
EBT-r3g2s1	1.35	0.83	818	32	0.46	3272
EBT-r3g3s1	2.14	0.56	871	81	0.43	2255
EBT-r3g4s1	1.85	0.63	844	62	0.39	2377
EBT-r3g5s1	1.67	0.66	803	58	0.45	3240
EBT-r3g6s1	1.50	0.76	825	39	0.53	3585
EBT-r3g7s1	1.59	0.71	828	51	0.41	3334
EBT-r3g8s1	2.35	0.53	902	80	0.44	963
EBT-r4g1s1	1.52	0.70	780	49	0.35	2399
EBT-r4g2s1	1.58	0.72	833	50	0.41	2289
EBT-r4g3s1	1.37	0.86	849	29	0.60	4949
EBT-r4g4s1	2.40	0.52	905	83	0.45	1287
EBT-r4g5s1	1.91	0.55	779	68	0.40	2253
EBT-r4g7s1	1.45	0.77	811	31	0.54	3578
Xenocrysts						
EBT-r2g3s1	362.57	0.99	228×10^3	4×10^3	0.19	1891
EBT-r2g4s1	363.62	0.99	229×10^3	3×10^3	0.19	1356
EBT-r4g6s1	344.47	0.99	216×10^3	3×10^3	0.18	1377
EBT-r4g8s1	358.28	0.99	224×10^3	4×10^3	0.17	1399
EBT-r4g9s1	359.50	0.99	226×10^3	3×10^3	0.36	1883
"*Early*" *Bishop Tuff F6 (061498-24-6)*[f]						
BTair-EBT-r7g2s1	1.12	0.96	781	21	0.62	4367
BTair-EBT-r8g1s3	0.99	0.94	698	26	0.34	3369
BTair-EBT-r8g2s2	1.12	0.98	792	18	0.62	5049
BTair-EBT-r8g10s3	1.27	0.94	864	28	0.56	4675

[a] Raw data.
[b] Fraction of radiogenic ^{206} Pb based on common ^{207} Pb/^{206} Pb correction.
[c] Ages corrected for initial ^{206} Pb and ^{238} U-series disequilibrium (see text for details).
[d] U concentrations are ~5% (1 σ) based on comparison to measurement of zircon standard 91500.
[e] Sample nomenclature after [30] and [33] for Glass Mountain domes and the Bishop Tuff, respectively. Analyses are identified by row (r#), grain (g#), spot (s#), near rim location ("rim"), and sessions in which an additional ~5–10 μm was removed by re-polishing ("pol").
[f] Replicate analyses of zircons previously analyzed [21].

References

[1] R.J. Arculus, Origins of the continental crust, J. Proc. R. Soc. N. S. W. 132 (1999) 83–110.

[2] H.R. Shaw, Links between magma–tectonic rate balances, plutonism, and volcanism, J. Geophys. Res. 90 (1985) 11275–11288.

[3] T.W. Sisson, C.R. Bacon, Gas-driven filter pressing in magmas, Geology 27 (1999) 613–616.

[4] O. Bachmann, G.W. Bergantz, On the origin of crystal-poor rhyolites: extracted from batholithic crystal mushes, J. Petrol. 45 (2004) 1565–1582.

[5] H.E. Huppert, R.S.J. Sparks, The generation of granitic magmas by intrusion of basalt into continental crust, J. Petrol. 29 (1988) 599–624.

[6] O. Bachmann, G.W. Bergantz, Rejuvenation of the Fish Canyon magma body: a window into the evolution of large-volume silicic magma systems, Geology 31 (2003) 789–792.

[7] A.K. Schmitt, J.I. Simon, Boron isotopic variations in hydrous rhyolitic melts: a case study from Long Valley, California, Contrib. Mineral. Petrol. 146 (2004) 590–605.

[8] D.S. Coleman, W. Gray, A.F. Glazner, Rethinking the emplacement and evolution of zoned plutons: geochronologic evidence for incremental assembly of the Tuolumne Intrusive Suite, California, Geology 32 (2004) 433–436.

[9] M.R. Reid, Timescales of magma transfer and storage in the crust, in: The Crust, R.L. Rudnick, ed., Treatise on Geochemistry 3, 2003, pp 167–194 (Elsevier Pergamon).

[10] C. Annen, R.S.J. Sparks, Effects of repetitive emplacement of basaltic intrusions on thermal evolution and melt generation in the crust, Earth Planet. Sci. Lett. 203 (2002) 937–955.

[11] A. Folch, J. Marti, The generation of overpressure in felsic magma chambers by replenishment, Earth Planet. Sci. Lett. 163 (1998) 301–314.

[12] D. Snyder, Thermal effects of the intrusion of basaltic magma into a more silicic magma chamber and implications for eruption triggering, Earth Planet. Sci. Lett. 175 (2000) 257–273.

[13] A.N. Halliday, A.E. Fallick, J. Hutchinson, W. Hildreth, A Nd, Sr, and O isotopic investigation into the causes of chemical and isotopic zonation in the Bishop Tuff, California, Earth Planet. Sci. Lett. 68 (1984) 379–391.

[14] J.M. Metz, G.A. Mahood, Development of the Long Valley, California, magma chamber recorded in precaldera rhyolite lavas of Glass Mountain, Contrib. Mineral. Petrol. 106 (1991) 379–397.

[15] J.N. Christensen, D.J. DePaolo, Time scales of large volume silicic magma systems: Sr isotopic systematics of phenocrysts and glass from the Bishop Tuff, Long Valley, California, Contrib. Mineral. Petrol. 113 (1993) 100–114.

[16] P. van den Bogaard, C. Schirnick, $^{40}Ar/^{39}Ar$ laser probe ages of Bishop Tuff quartz phenocrysts substantiate long-lived silicic magma chamber at Long Valley, United States, Geology 23 (1995) 759–762.

[17] I.N. Bindeman, J.W. Valley, Oxygen isotope study of the Long Valley magma system, California: isotope thermometry and convection in large silicic magma bodies, Contrib. Mineral. Petrol. 144 (2002) 185–205.

[18] G.R. Davies, A.N. Halliday, G.A. Mahood, C.M. Hall, Isotopic constraints on the production rates, crystallisation histories and residence times of pre-caldera silicic magmas, Long Valley, California, Earth Planet. Sci. Lett. 125 (1994) 17–37.

[19] G.R. Davies, A.N. Halliday, Development of the Long Valley rhyolitic magma system: strontium and neodymium isotope evidence from glasses and individual phenocrysts, Geochim. Cosmochim. Acta 62 (1998) 3561–3574.

[20] J.N. Christensen, A.N. Halliday, Rb–Sr ages and Nd isotopic compositions of melt inclusions from the Bishop Tuff and the generation of silicic magma, Earth Planet. Sci. Lett. 144 (1996) 547–561.

[21] M.R. Reid, C.D. Coath, In situ U–Pb ages of zircons from the Bishop Tuff: no evidence for long crystal residence times, Geology 28 (2000) 443–446.

[22] W. Hildreth, The magma chamber of the Bishop Tuff: gradients in temperature, pressure, and composition, Ph.D., University of California, Berkeley, 1977.

[23] W. Hildreth, The Bishop Tuff: evidence for the origin of compositional zonation in silicic magma chambers, Geol. Soc. Am., Spec. Pap. 180 (1979) 43–76.

[24] A.N. Halliday, G.A. Mahood, P. Holden, J.M. Metz, T.J. Dempster, J.P. Davidson, Evidence for long residence times of rhyolitic magma in the Long Valley magmatic system: the isotopic record in precaldera lavas of Glass Mountain, Earth Planet. Sci. Lett. 94 (1989) 274–290.

[25] R.L. Hervig, N.W. Dunbar, Cause of chemical zoning in the Bishop (California) and Bandelier (New Mexico) magma chambers, Earth Planet. Sci. Lett. 111 (1992) 97–108.

[26] A.T. Anderson, A.M. Davis, F. Lu, Evolution of Bishop Tuff rhyolitic magma based on melt and magnetite inclusions and zoned phenocrysts, J. Petrol. 41 (2000) 449–473.

[27] E.B. Watson, T.M. Harrison, Zircon saturation revisited: temperature and composition effects in a variety of crustal magma types, Earth Planet. Sci. Lett. 64 (1983) 295–304.

[28] M.R. Reid, C.D. Coath, T.M. Harrison, K.D. McKeegan, Prolonged residence times for the youngest rhyolites associated with Long Valley Caldera: ^{230}Th–^{238}U ion microprobe dating of young zircons, Earth Planet. Sci. Lett. 150 (1997) 27–39.

[29] C.D. Rinehart, D.C. Ross, Geology and mineral deposits of the Mount Morrison quadrangle, Sierra Nevada, California, with a section on a gravity study of Long Valley by L.C. Pakiser, U.S., Geol. Surv. Prof. Pap. 385 (1957) 104.

[30] J.M. Metz, G.A. Mahood, Precursors to the Bishop Tuff eruption: Glass Mountain, Long Valley, California, J. Geophys. Res. 90 (1985) 11,121–11,126.

[31] J.M. Metz and R.A. Bailey, Geologic map of Glass Mountain, Mono Country, California, U.S. Geological Survey Map I-1995, 1993.

[32] W. Hildreth, Gradients in silicic magma chambers: implications for lithospheric magmatism, J. Geophys. Res. 86 (1981) 10153–10192.

[33] C.J.N. Wilson, W. Hildreth, The Bishop Tuff: new insights from eruptive stratigraphy, J. Geol. 105 (1997) 407–439.
[34] X. Quidelleur, M. Grove, O.M. Lovera, T.M. Harrison, A. Yin, Thermal evolution of slip history of the Renbu Zedong Thrust, southeastern Tibet, J. Geophys. Res. 102 (1997) 2659–2679.
[35] J.M. Mattinson, Anomalous isotopic composition of lead in young zircons, Year B-Carnegie Inst. Wash. 72 (1973) 616–623.
[36] U. Schärer, The effect of initial ^{230}Th disequilibrium on young U–Pb ages: the Makalu case, Himalaya, Earth Planet. Sci. Lett. 67 (1984) 191–204.
[37] M.K. Reagan, K.W.W. Sims, J. Erich, R.B. Thomas, H. Cheng, R.L. Edwards, G.D. Layne, L. Ball, Time-scales of differentiation from mafic parents to rhyolite in North American continental arcs, J. Petrol. 44 (2003) 1703–1726.
[38] J. Davidson, F. Tepley III and K.M. Knesel, Isotopic fingerprinting may provide insight into evolution of magmatic systems, Eos, Transactions, American Geophysical Union 79, 185, 189, 193, (1998).
[39] D. York, Least-squares fitting of a straight line with correlated errors, Earth Planet. Sci. Lett. 5 (1969) 320–324.
[40] K.I. Mahon, The "New York" regression: application of an improved statistical method to geochemistry, Int. Geol. Rev. 38 (1996) 293–303.
[41] J.M. Metz and G.A. Mahood, Eruptive history of Glass Mountain, Long Valley, California: precursors to a large explosive eruption, Open-File Report-U.S. Geological Survey Report: OF 84-0939, 41–75, (1984).
[42] D.J. Cherniak, E.B. Watson, A study of strontium diffusion in K-feldspar, Na–K feldspar and anorthite using Rutherford backscattering spectroscopy, Earth Planet. Sci. Lett. 113 (1992) 411–425.
[43] D.J. Cherniak, E.B. Watson, Pb diffusion in zircon, Chem. Geol. 172 (2000) 5–24.
[44] F. Lu, A.T. Anderson, A.M. Davis, Melt inclusion and crystal–liquid separation in rhyolitic magma of the Bishop Tuff, Contrib. Mineral. Petrol. 110 (1992) 113–120.
[45] J. Vazquez, M.R. Reid, Time scales of magma storage and differentiation of voluminous high-silica rhyolites at Yellowstone caldera, Wyoming, Contrib. Mineral. Petrol. 144 (2002) 274–285.
[46] J.A. Wolff, F.C. Ramos, J.P. Davidson, Sr isotope disequilibrium during differentiation of the Bandelier Tuff: constraints on the crystallization of a large rhyolitic magma chamber, Geology 27 (1999) 495–498.
[47] J.A. Wolff, F.C. Ramos, Pb isotope variations among Bandelier Tuff feldspar: no evidence for a long-lived silicic magma chamber, Geology 31 (2003) 533–536.
[48] R.G. Gibson, M.T. Naney, Textural development of mixed, finely porphyritic silicic volcanic rocks, Inyo Domes, Eastern California, J. Geophys. Res. 97 (1992) 4541–4559.
[49] N.W. Dunbar, R.L. Hervig, Petrogenesis and volatile stratigraphy of the Bishop Tuff: evidence from melt inclusion analysis, J. Geophys. Res. 97 (1992) 15,129–15,150.
[50] J.W. Boyce, M. Grove, M.R. Reid, Experimental evidence for the non-retentive behavior of Ar from melt inclusions in quartz phenocrysts, Eos., Transactions, American Geophysical Union 80 (1999) F1130.
[51] J.A. Winick, W.C. McIntosh, N.W. Dunbar, Melt-inclusion-hosted excess ^{40}Ar in quartz crystals of the Bishop and Bandelier magma systems, Geology 29 (2001) 275–278.
[52] S.J.A. Brown, I.R. Fletcher, SHRIMP U–Pb dating of the preeruption growth history of zircons from the 340 ka Whakamaru Ignimbrite, New Zealand: Evidence for >250 k.y. magma residence times, Geology 27 (1999) 1035–1038.
[53] C.R. Bacon, H.M. Persing, J.L. Wooden, T.R. Ireland, Late Pleistocene granodiorite beneath Crater Lake caldera, Oregon, dated by ion microprobe, Geology 28 (2000) 467–470.
[54] W.A. Duffield, J. Ruiz, J.D. Webster, Roof-rock contamination of magma along the top of the reservoir for the Bishop Tuff, J. Volcanol. Geotherm. Res. 69 (1995) 187–195.
[55] A. Heumann, G.R. Davies, U–Th disequilibrium and Rb–Sr age constraints on the magmatic evolution of peralkaline rhyolites from Kenya, J. Petrol. 43 (2002) 557–577.
[56] A.H. Heumann, G.R. Davies, T. Elliott, Crystallization history of rhyolites at Long Valley, California, inferred from combined U-series and 28 Rb–Sr isotope systematics, Geochim. Cosmochim. Acta 66 (2002) 1821–1837.
[57] P.J. Wallace, A.T. Anderson, A.M. Davies, Gradients in H_2O, CO_2, and exsolved gas in a large-volume silicic magma system: interpreting the record preserved in melt inclusions from the Bishop Tuff, J. Geophys. Res. 104 (1999) 20,097–20,122.
[58] P.J. Michael, Chemical differentiation of the Bishop Tuff and other high-silica magmas through crystallization processes, Geology 11 (1983) 31–34.
[59] B.T. Peppard, I.M. Steele, A.M. Davies, P.J. Wallace, A.T. Anderson, Zoned quartz and phenocrysts from the rhyolitic Bishop Tuff, Am. Mineral. 86 (2001) 1034–1052.
[60] I.N. Bindeman, Crystal sizes in evolving silicic magma chambers, Geology 31 (2003) 367–370.
[61] C.H. Langmuir, Geochemical consequences of in situ crystallization, Nature 340 (1989) 199–205.
[62] R.A. Bailey, G.B. Dalrymple, M.A. Lanphere, Volcanism, structure, and geochronology of Long Valley caldera, Mono Country, California, J. Geophys. Res. 81 (1976) 725–744.
[63] B.L.A. Charlier, D.W. Peate, C.J.N. Wilson, J.B. Lowenstern, M. Storey, S.J.A. Brown, Crystallisation age in coeval silicic magma bodies: ^{238}U–^{230}Th disequilibrium evidence from the Rotoiti and Earthquake Flat eruption deposits, Taupo Volcanic Zone, New Zealand, Earth Planet. Sci. Lett. 206 (2003) 441–457.
[64] C.J.N. Wilson, W. Hildreth, Hybrid fall deposits in the Bishop Tuff, California: a novel pyroclastic depositional mechanism, Geology 26 (1998) 7–10.